ELSEVIER

Journal of Chromatography A, 834 (1999) 445–452

JOURNAL OF CHROMATOGRAPHY A

Separation of micrometer-size oxide particles by capillary zone electrophoresis

Steven L. Petersen*, Nathan E. Ballou

Environmental and Health Sciences Division, Pacific Northwest National Laboratory, P.O. Box 999, Mailstop P7-07, Richland, WA 99352, USA

Abstract

High quality separations of three-component mixtures of suspended micrometer-size metal oxide particles have been achieved by capillary zone electrophoresis in two different high-pH aqueous buffer systems. Mixtures of Al_2O_3, Fe_3O_4 and TiO_2 and of Al_2O_3, Fe_3O_4 and Fe_2O_3 were separated in 5–10 min in either carbonate buffer, pH 10.6 or pyrophosphate buffer, pH 10.2. The effects of electric field strength, buffer concentration and buffer type on separation quality were determined. Under optimized conditions, the separations were nearly baseline resolved. Complete separation of a mixture of Al_2O_3 and UO_2 particles was also accomplished. Different sized particles/aggregates of a given oxide were found to co-migrate so that, for the systems studied, particle size effects were negligible and the separations were electrophoretic in nature. Reproducibilities of migration times and peak widths, heights and shapes were found to be excellent, with relative standard deviations of migration times consistently being $<1\%$. Published by Elsevier Science B.V.

Keywords: Buffer composition; Metal oxides

1. Introduction

The first reported separations of non-biological particulate species by capillary zone electrophoresis (CZE) were of mixtures of charged polystyrene latex particles [1–4]. These reports have been followed by a number of publications demonstrating the potential of CZE for the characterization and/or separation of inorganic particles [5–11]. Some of these more recent reports have also included additional studies on latex particle separation and characterization by CZE [6,7]. Examples of CZE studies of inorganic particles include the separation and characterization of colloidal silica [5], the characterization of thorium phosphate and metal oxide colloids [6,7], the separation of latex and thorium phosphate colloids [7], the separation of silica-based and polyanaline-based composite particles [10], and the characterization of gold nanoparticles [11].

Two recent publications from this laboratory have described the characterization and separation of metal oxide particles by CZE in inert electrolyte systems [8] and in three aqueous buffer systems ranging in pH from 6.8 to 10.1 [9]. This paper describes the results of optimization studies for separations of the same metal oxides studied previously [8,9] in two different high-pH buffer systems.

2. Experimental

2.1. Apparatus

All experiments were performed on a P/ACE 2000

*Corresponding author. Fax: +1-509-376-5021, E-mail: steven.petersen@pnl.gov

0021-9673/99/$ – see front matter Published by Elsevier Science B.V.
PII: S0021-9673(98)00864-4

automated capillary electrophoresis instrument (Beckman Instruments, Palo Alto, CA, USA) using 96 μm I.D.×355 μm O.D., fused-silica capillaries (Polymicro Technologies, Phoenix, AZ, USA), which were thermostatted to 25.0±0.1°C. For runs employing UO_2 particles, the capillary had an effective length of 30.5 cm and a total length of 37.2 cm. For all other runs, the capillary had an effective length of 30.3 cm and a total length of 37.0 cm. The suspended particles were detected turbidimetrically at 254 nm using the instrument's UV absorbance detector. The width of the detector aperture (along the capillary's axis) was 200 μm.

2.2. Preparation of buffers and oxide particle suspensions

Pyrophosphate buffers of various concentrations were prepared from reagent-grade sodium pyrophosphate (Fisher Scientific, Fair Lawn, NJ, USA) and Milli-Q deionized water (Millipore, Bedford, MA, USA). Carbonate buffer solutions of various concentrations and carbonate–hydrogencarbonate (3.00:1) were prepared from sodium carbonate (Aldrich, Milwaukee, WI, USA), sodium hydrogencarbonate (Aldrich), and deionized water. The pyrophosphate buffers had a pH of 10.2±0.1 and the carbonate buffers had a pH of 10.6±0.1. Running buffer solutions were filtered daily using syringe filters with a pore size of 0.2 μm. Buffer concentrations reported below refer to the total concentration of all forms of the buffer anion.

Individual stock suspensions of commercially-available oxide particles were quantitatively prepared from the oxide powders (Polysciences, Warrington, PA, USA and AESAR/Johnson Matthey, Ward Hill, MA, USA) and various pyrophosphate and carbonate buffer solutions. The concentration of the oxide particles in the stock suspensions was 0.15% (v/v). For CZE runs, individual oxide particle standards and oxide particle standard mixtures were prepared by quantitative dilution of the stock suspension(s) into the corresponding buffer solutions. The concentration of each oxide in the standards and mixtures was typically 0.015% (v/v). Stock suspensions of 100 ppm UO_2 in carbonate buffers were prepared from a natural UO_2 powder obtained from the Environmental and Health Sciences Division of Pacific Northwest National Laboratory (PNNL). In all cases, particle standards and mixtures were prepared with buffer concentrations matching those of the corresponding running buffers. The nominal particle diameter and source of each of the oxides employed in this work are summarized in Table 1. It should be noted that all of the oxides aggregated to various extents in the carbonate and pyrophosphate buffer suspensions, such that the average size of electrophoresing particles was in the micrometer range.

2.3. Procedure

At the beginning of each day, the capillary was conditioned by rinsing it with 0.1 *M* NaOH, deionized water, and running buffer for 15 min each. After conditioning, the capillary was allowed to contact running buffer only. Normal system performance was then verified by measuring the electroosmotic flow (EOF) rate using acetone (0.5%, v/v in the running buffer) as the neutral marker. Particle standards and mixtures were initially ultrasonicated for 5 min to enhance dispersion. Then, prior to each run, the particle suspensions were agitated by hand to ensure that all particles were suspended. Hydrodynamic (pressure) injections were employed to inject the particle suspensions at the anode end of the capillary. Sample plug lengths were typically equal to 1.0% of the total capillary length. The runs were performed under constant voltage using normal polarity and applied electric field strengths of 100–500 V/cm. Between runs, the capillary was rinsed with 20 capillary volumes of running buffer. The volume levels in the anode and cathode vials were carefully monitored and adjusted as necessary to maintain equivalent levels and thus prevent gravity flow of buffer through the capillary during the course

Table 1
Nominal diameters and sources of oxide particles

Oxide	Nominal diameter (μm)	Source
γ-Al_2O_3	0.01	AESAR
γα-Al_2O_3	0.3	AESAR
Fe_3O_4	0.2	Polysciences
Fe_2O_3	0.3–0.8	Polysciences
TiO_2	0.45	Polysciences
UO_2	0.2–13	PNNL

of a CZE run. At the end of each day, the capillary was thoroughly rinsed with deionized water.

3. Results and discussion

3.1. Influence of electric field strength on separation quality

The effect of electric field strength, *E*, on separation quality was studied for three systems consisting of the mixtures γα-Al_2O_3–Fe_3O_4–TiO_2 and γα-Al_2O_3–Fe_3O_4–Fe_2O_3 in 5.00 m*M* carbonate buffer, pH 10.6 and the mixture γ-Al_2O_3–Fe_3O_4–TiO_2 in 2.19 m*M* pyrophosphate buffer, pH 10.2. Each oxide mixture component was present at a concentration of 0.015% (v/v). Separations of each of the three-component mixtures were performed in duplicate at $E=200$, 300, 400 and 500 V/cm. Selectivity, efficiency and resolution were calculated in the standard manner [4] for the 24 resulting runs. Representative electropherograms are shown in Fig. 1 for the γα-Al_2O_3–Fe_3O_4–TiO_2 mixture in 5.00 m*M* carbonate buffer, pH 10.6. Note that the *x*-axis has been converted from migration time to apparent mobility so that the effect of *E* on apparent mobility, selectivity and efficiency can more readily be observed. The term ''apparent mobility'' refers to the sum of the electroosmotic and electrophoretic mobilities.

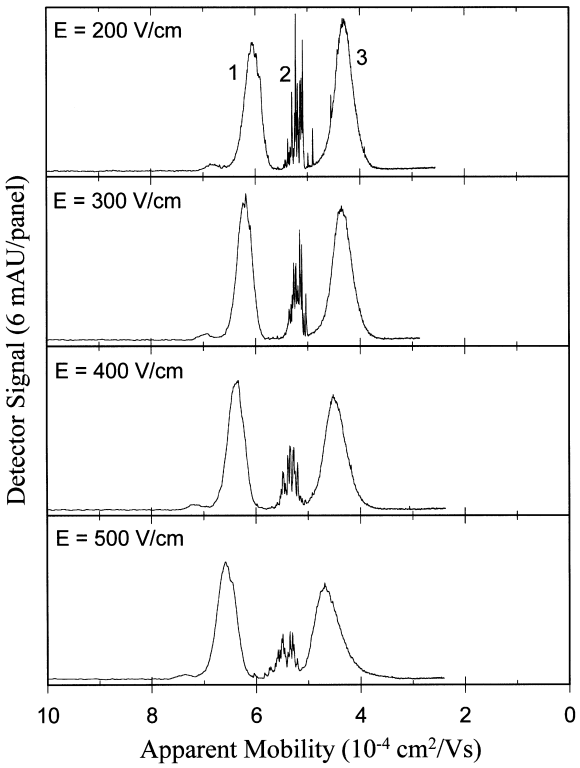

Fig. 1. Capillary zone electrophoretic separations at four electric field strengths of a mixture containing 0.015% (v/v) each of γα-Al_2O_3 (1), Fe_3O_4 (2) and TiO_2 (3) particles in 5.00 m*M* carbonate buffer, pH 10.6. The *x*-axis has been converted from units of migration time to apparent mobility (see Section 3.1).

All three systems yielded the same conclusions. Selectivities were found to be independent of *E*, in accord with theory and with results previously obtained for chemically-modified latex particles [4]. Efficiencies were constant at $E=200$–300 V/cm, but decreased by an average of 41% on going from $E=300$ V/cm to $E=500$ V/cm. As can be seen in Fig. 1, apparent mobilities increased with *E*, most noticeably at $E>300$ V/cm. The apparent mobilities increased an average of 3.0% on going from $E=200$ V/cm to $E=500$ V/cm. The efficiency and apparent mobility trends are suggestive of inadequate dissipation of Joule heat at $E>300$ V/cm, which was confirmed by Ohm's Law plots for the three systems, which all showed deviation from linearity at $E>300$ V/cm. The large efficiency losses at high *E* are consistent with the susceptibility of slow-diffusing micrometer-size particles to the thermal Taylor dispersion caused by the parabolic velocity profile that develops across the capillary due to Joule heating [12,13]. Although separation quality did not appear to be significantly degraded at $E=500$ V/cm relative to $E=300$ V/cm (Fig. 1), subsequent separations were performed at $E\leq 300$ V/cm to ensure maximum efficiency. For the capillary dimensions and instrument employed in this work, this translates to a maximum operating power of 0.75 W per m of capillary length.

3.2. Influence of buffer concentration on separation quality

The effect of buffer concentration on CZE separation quality was studied for two three-component oxide particle mixtures in both carbonate and pyrophosphate buffers. Representative results are shown

in Figs. 2 and 3. Fig. 2 shows separations of the mixtures γα-Al_2O_3–Fe_3O_4–TiO_2 (A) and γα-Al_2O_3–Fe_3O_4–Fe_2O_3 (B) at $E=300$ V/cm in 2.50, 5.00 and 10.0 m*M* carbonate buffer, pH 10.6. Fig. 3 shows separations of the mixtures γ-Al_2O_3–Fe_3O_4–TiO_2 (A) and γ-Al_2O_3–Fe_3O_4–Fe_2O_3 (B) at $E=300$ V/cm in 1.09, 2.19 and 4.38 m*M* pyrophosphate buffer, pH 10.2. As was done for the electric field strength studies, CZE runs of individual oxide standards were used for the identification of peaks in the mixture electropherograms. Good agreement was obtained between the migration times observed for the standards and mixtures, the average difference being less than 2%, suggesting that co-aggregation of the different types of oxide particles in the mixtures was not significant. The minor peak for Fe_2O_3 (Fig. 3B) has not been identified and may be due to an impurity. The pyrophosphate buffer concentrations were chosen to match the Na^+ concentrations of the corresponding carbonate buffers, since, in the absence of specific adsorption, the dependence of electrophoretic mobility on buffer concentration is predominantly determined by the valence and concentration of the counterion [14,15]. Selectivity, efficiency and resolution values were again calculated and analyzed for the data in Figs. 2 and 3.

As is shown by Figs. 2 and 3, all selectivities between different types of oxide particles increased significantly with increasing buffer concentration. On average, selectivities increased by 64% on going from the lowest to highest buffer concentrations. The calculated electrophoretic mobilities showed no consistent trend with buffer concentration, which is consistent with previously reported results for these same oxides in three other buffer systems and suggests significant interaction of the buffer anions with the particle surfaces [9]. Electroosmotic mobilities did, however, consistently decrease with increasing buffer concentration and thus caused selectivities to increase with increasing buffer con-

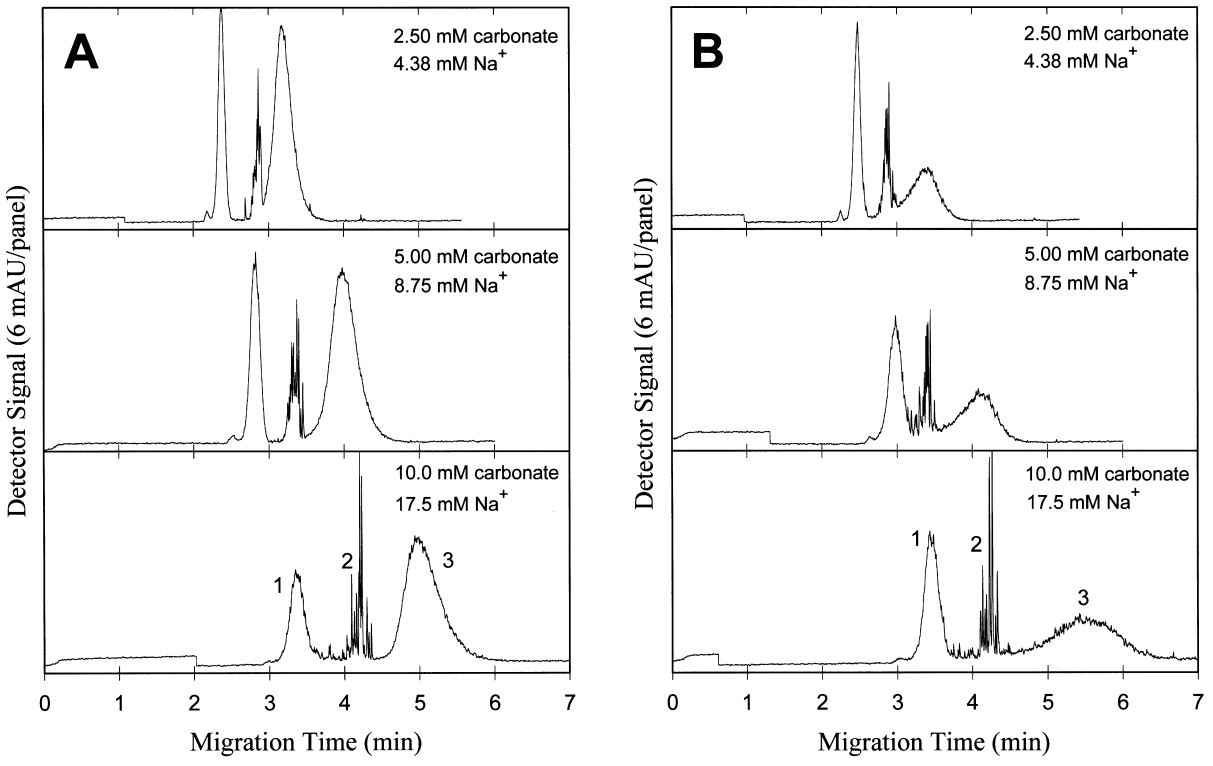

Fig. 2. Capillary zone electrophoretic separations at three concentrations of carbonate buffer, pH 10.6, of mixtures containing 0.015% (v/v) each of (A) γα-Al_2O_3 (1), Fe_3O_4 (2) and TiO_2 (3) and (B) γα-Al_2O_3 (1), Fe_3O_4 (2) and Fe_2O_3 (3) particles. The electric field strength was 300 V/cm for all separations.

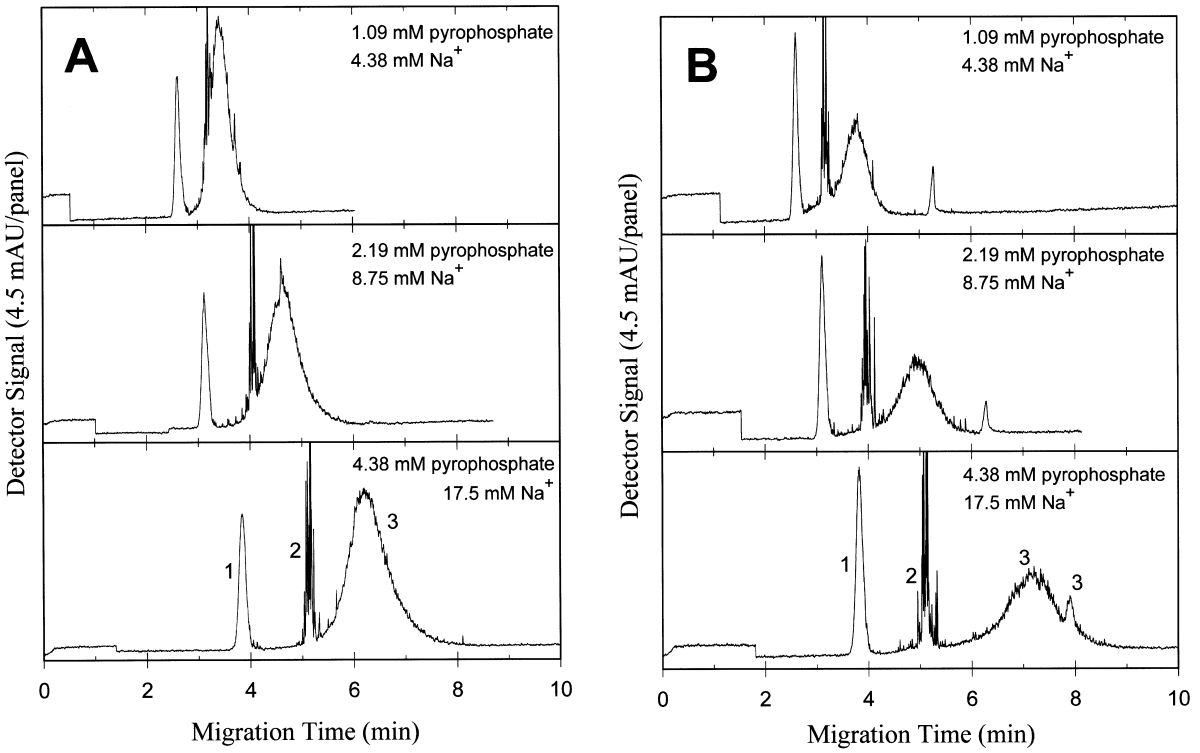

Fig. 3. Capillary zone electrophoretic separations at three concentrations of pyrophosphate buffer, pH 10.2, of mixtures containing 0.015% (v/v) each of (A) γ-Al_2O_3 (1), Fe_3O_4 (2) and TiO_2 (3) and (B) γ-Al_2O_3 (1), Fe_3O_4 (2) and Fe_2O_3 (3) particles. The electric field strength was 300 V/cm for all separations.

centration in the manner described by Jorgenson and Lukacs [16].

Figs. 2 and 3 appear to show that the quality of CZE separations of oxide particles increases with increasing buffer concentration. This is true for the mixtures separated in pyrophosphate buffer, where efficiencies showed no significant trend with changing buffer concentration. The efficiencies for the γ-Al_2O_3, TiO_2 and Fe_2O_3 peaks averaged 3820±180, 410±77 and 320±18 theoretical plates, respectively, in the pyrophosphate buffers. Efficiencies were not measured for the noisy Fe_3O_4 peaks. These low efficiencies for the oxide particle zones are most likely due to microheterogeneity in the samples as previously observed for chemically-modified latex particles [4]. The independence of efficiency and dependence of selectivity on pyrophosphate buffer concentration resulted in resolutions that increased from 3.11±0.05 to 5.52±0.08 between the γ-Al_2O_3 and TiO_2 peaks (Fig. 3A) and from 4.20±0.11 to 6.92±0.01 between the γ-Al_2O_3 and Fe_2O_3 peaks (Fig. 3B) on going from 1.09 m*M* to 4.38 m*M* pyrophosphate.

The highest quality separations in carbonate buffer also appear to be at the highest buffer concentration, where baseline resolution of each of the three-component oxide particle mixtures was achieved (Fig. 2). Efficiencies, however, were found to decrease by an average factor of 2.2 on going from 2.50 m*M* to 10.0 m*M* carbonate. These efficiency losses more than offset the selectivity gains with increasing buffer concentration such that the highest resolutions were actually obtained at the lowest carbonate buffer concentration. The dependence of efficiency on carbonate buffer concentration is thought to be the result of higher dispersibility, and thus a lower degree of microheterogeneity, at lower carbonate buffer concentrations. The efficiencies for the γα-Al_2O_3, TiO_2 and Fe_2O_3 peaks were 3610±150, 890±10 and 410±10 theoretical plates, respectively,

in the 2.50 m*M* carbonate buffer. The observed resolutions in the 2.50 m*M* carbonate buffer were 3.39±0.04 between the γα-Al_2O_3 and TiO_2 peaks (Fig. 2A) and 3.56±0.07 between the γα-Al_2O_3 and Fe_2O_3 peaks (Fig. 2B). These resolutions decreased by an average of 9.4% on going from 2.50 m*M* to 10.0 m*M* carbonate. Although the calculated resolutions were highest in the 2.50 m*M* carbonate buffer, the 10.0 m*M* carbonate buffer would obviously be the better system for collection of purified particle fractions (Fig. 2). Note that resolution comparisons between the two buffer types are not possible for the work reported here, since different aluminas were used in the different buffer types as described in Section 3.3.

3.3. Influence of buffer type on selectivity

The data in Figs. 2 and 3 also reveal that buffer type can have a significant effect on the selectivity observed between given oxides. Comparison of Fig. 2A with Fig. 3A, for example, shows that the selectivity between Fe_3O_4 and TiO_2 is higher in carbonate buffer than in pyrophosphate buffer. Another example is that γα-Al_2O_3 and Fe_3O_4 are easily separated in carbonate buffer (Fig. 2), whereas these two oxides co-migrate in pyrophosphate buffer (not shown). A final example, is the behavior of the minor Fe_2O_3 peak, which is shown in Fig. 3B to elute after the major Fe_2O_3 peak. However, in carbonate buffer, this minor peak elutes before the major peak and is obscured in Fig. 2B because it co-migrates with the Fe_3O_4 peak. These examples demonstrate that buffer type can be used as a tool in enhancing the quality of a particular oxide particle separation.

3.4. Particle size effects

Table 1 lists the nominal particle diameters specified by the manufacturers for the commercial oxide powders and the diameter for the UO_2 particles, which was determined at PNNL by electron microscopy. Sedimentation studies and visual observations of the oxide particle suspensions indicated that the particles were not fully dispersed as singles, but rather were present as aggregates of varying and undetermined size. However, experiments with UO_2 and Fe_3O_4 have shown that, for each of the oxides, large aggregates co-migrated with small aggregates and any single particles that were present.

Fig. 4 shows the CZE separation of a mixture containing 17 ppm γα-Al_2O_3 and 83 ppm UO_2 particles in 6.00 m*M* carbonate buffer, pH 10.6 at $E=185$ V/cm. The UO_2 peak in the top electropherogram is due to both coarse and fine UO_2 particles, with a total size range of 0.2–13 μm. The UO_2 peak in the bottom electropherogram is due only to the fine UO_2 particles, which have a size range of 0.2–0.5 μm. The size ranges for the coarse and fine UO_2 particles were determined by electron microscopy. Practical experience has shown that small aggregates and single particles yield smooth peaks, whereas large aggregates result in spikes that ride on the main (smooth) peak. Thus, comparison of

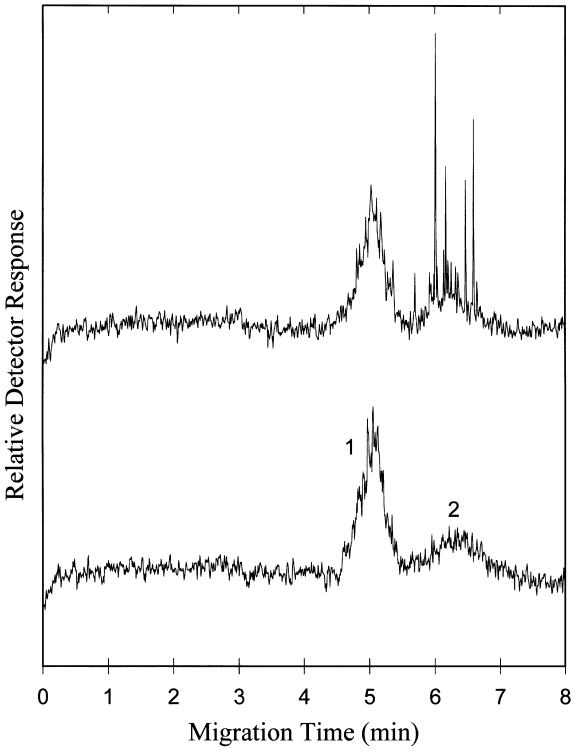

Fig. 4. Capillary zone electrophoretic separations of a mixture containing 17 ppm γα-Al_2O_3 (1) and 83 ppm UO_2 (2) particles in 6.00 m*M* carbonate buffer, pH 10.6. The electric field strength was 185 V/cm. The electropherograms are from mixtures containing all UO_2 particles (top) and containing only those UO_2 particles that remained suspended for >4 h (bottom).

the two electropherograms in Fig. 4 verifies that the large UO_2 aggregates co-migrate with the small aggregates and any single particles present.

This same behavior has been demonstrated for Fe_3O_4 as shown in Fig. 5. The suspensions of Fe_3O_4 used for this work had aggregates that varied in size from those that remained dispersed for many hours to large visible aggregates that settled-out in just a few minutes. The top electropherogram in Fig. 5 is due to all Fe_3O_4 particles, while the bottom electropherogram is due only to the fine particles that remained suspended for >60 min. Comparison of the two electropherograms in Fig. 5 verifies that the coarse and fine Fe_3O_4 particles co-migrate. For the mixtures containing Fe_3O_4, all Fe_3O_4 particles were injected as is evident by the spiky Fe_3O_4 peaks in Figs. 1–3.

The observed independence of migration time on particle size for UO_2 and Fe_3O_4 is consistent with theoretical expectations for particles in the micrometer size range [17,18] and is encouraging for the development of routine CZE methods for the separation of particles according to their chemical nature. The co-migration of large and small aggregates suggests that sedimentation and particle–wall interaction effects are insignificant compared to electrokinetic effects so that the CZE separations of oxide particles are truly electrophoretic in nature.

3.5. Reproducibility

The run-to-run reproducibility of the electropherograms for CZE separations of oxide particles has been found to be as good as that typically obtained for ionic analytes. For the electric field strength and buffer concentration studies reported

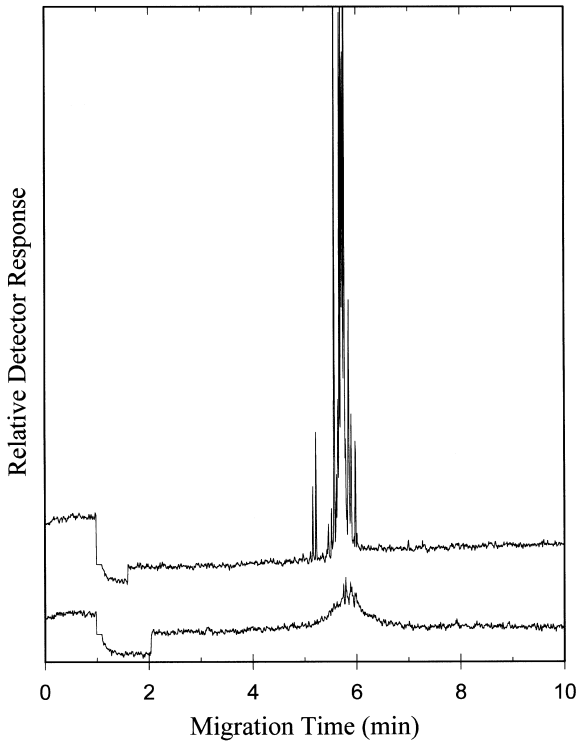

Fig. 5. Capillary zone electrophoretic runs of a 0.014% (v/v) Fe_3O_4 standard in 6.00 m*M* carbonate buffer, pH 10.6. The electric field strength was 185 V/cm. The electropherograms are from injections of all particles (top) and of only the fine particles that remained suspended for >60 min (bottom).

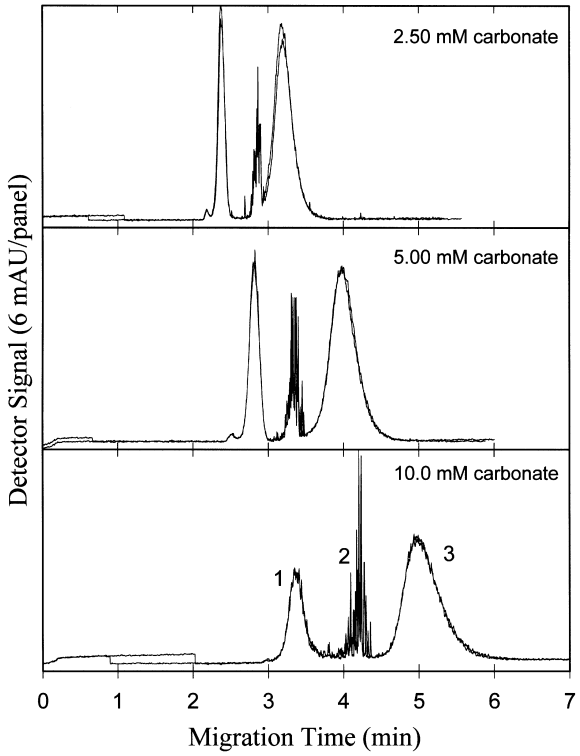

Fig. 6. Capillary zone electrophoretic separations at three concentrations of carbonate buffer, pH 10.6, of mixtures containing 0.015% (v/v) each of γα-Al_2O_3 (1), Fe_3O_4 (2) and TiO_2 (3) particles. The electric field strength was 300 V/cm for all separations. Duplicate runs are displayed in each panel.

here, the relative average deviations of the migration times for the duplicate runs performed under 24 different sets of conditions (72 peaks analyzed) ranged from 0.00% to 0.81% and averaged 0.26%. In a similar study not reported on here, for triplicate runs of nine different three-component oxide particle mixtures, the relative standard deviations (R.S.D.s) of the migration times for the 27 peaks ranged from 0.1% to 1.2% and averaged 0.44%. In consideration of the limited stability of the oxide particle suspensions, the reproducibility of migration times from run-to-run was excellent. For triplicate runs of the UO_2 standard in 6.00 m*M* carbonate buffer, pH 10.6, the R.S.D. of the migration time was 0.092% for runs in which both the coarse and fine UO_2 particles were injected and 0.69% when only the fine UO_2 particles were injected. A final example of the excellent reproducibility of the electropherograms for CZE separations of oxide particles is given in Fig. 6, which is the same as Fig. 2A except that duplicate runs are plotted at each buffer concentration. The overlay plots in Fig. 6 demonstrate the excellent reproducibility in peak width, peak height, peak shape and migration time that was typically observed for CZE separations of oxide particle mixtures.

Acknowledgements

This work was supported by the US Department of Energy. Pacific Northwest National Laboratory is operated for the US Department of Energy by Battelle Memorial Institute under Contract DE-AC06-76RLO 1830.

References

[1] B.B. VanOrman, G.L. McIntire, J. Microcol. Sep. 1 (1989) 289.
[2] B.B. VanOrman, G.L. McIntire, Am. Lab. November (1990) 66.
[3] H.K. Jones, N.E. Ballou, Anal. Chem. 62 (1990) 2484.
[4] S.L. Petersen, N.E. Ballou, Anal. Chem. 64 (1992) 1676.
[5] R.M. McCormick, J. Liq. Chromatogr. 14 (1991) 939.
[6] B. Fourest, N. Hakem, R. Guillaumont, Radiochim. Acta 66–67 (1994) 173.
[7] B. Fourest, N. Hakem, J. Perrone, R. Guillaumont, J. Radioanal. Nuclear Chem. 208 (1996) 309.
[8] C. Quang, S.L. Petersen, G.R. Ducatte, N.E. Ballou, J. Chromatogr. A 732 (1996) 377.
[9] G.R. Ducatte, S.L. Petersen, N.E. Ballou, J. Microcol. Sep. 8 (1996) 403.
[10] J. Janca, S.L. Hen, M. Spirkova, J. Stejskal, J. Microcol. Sep. 9 (1997) 303.
[11] U. Schnabel, C.-H. Fischer, E. Kenndler, J. Microcol. Sep. 9 (1997) 529.
[12] E. Grushka, R.M. McCormick, J.J. Kirkland, Anal. Chem. 61 (1989) 241.
[13] W.A. Gobie, C.F. Ivory, J. Chromatogr. 516 (1990) 191.
[14] W.G. Eversole, W.W. Boardman, J. Chem. Phys. 9 (1941) 798.
[15] R.J. Hunter, H.J.L. Wright, J. Colloid Interface Sci. 37 (1971) 564.
[16] J.W. Jorgenson, K.D. Lukacs, Anal. Chem. 53 (1981) 1298.
[17] R.J. Hunter, Zeta Potential in Colloid Science, Academic Press, London, 1981, Ch. 3.
[18] H. Ohshima, J. Colloid Interface Sci. 168 (1994) 269.